

The effect of thermal losses on traveling waves for in-situ combustion in porous medium

G. Chapiro¹ and D. Marchesin²

¹ Universidade Federal de Juiz de Fora, Juiz de Fora, MG 36036-900, Brazil

² Instituto de Matemática Pura e Aplicada, Rio de Janeiro, RJ 22460-320, Brazil.

E-mail: grigori@ice.ufjf.br

Abstract. This paper is motivated by a model for the injection of air into an underground porous medium that contains a solid fuel, taking into account thermal losses to the surrounding rock. In our previous works the model was simplified and all wave sequences for the Riemann problem solution were obtained. Additionally, a rigorous proof of the existence of the traveling wave solution was presented. Taking thermal losses into account is important from a physical point of view because they play an important role, especially in the laboratory experiments.

In this work the first step is made to understand the effect of heat losses. The model is modified by including the thermal losses term, making it more physically realistic. In order to simplify the proof of the existence and uniqueness of the traveling wave solution, we disregard diffusion effects and the dependence of gas density on temperature. Some numerical examples are presented to illustrate the theoretical study.

1. Introduction

Air injection with in-situ combustion offers several potential technical and economic advantages that may include faster oil production, reduced operational costs and increased CO_2 content with decreased oil viscosity. The engineering of the process is more difficult than any other method of crude oil recovery, but the advantages of in-situ combustion motivate researchers to investigate it. Despite other difficulties related to engineering and chemical modeling, solving the equations for such models is a challenge.

This paper is part of long term research project the purpose of which is to identify waves that arise in one-dimensional models of combustion in porous media, and to understand how the waves fit together in solutions of Riemann problems; see [1, 2, 3, 4, 5, 6, 7, 8], and references therein.

The paper is motivated by a model for the injection of air into a porous medium that contains oil so viscous that it can be considered a solid fuel. The model was proposed in [9] and further studied in [2]. This model was simplified in [10] in order to (i) reproduce the variety of phenomena observed when air is injected into a porous medium containing a solid fuel, yet (ii) to be simple enough to permit a rigorous investigation. This simplification facilitates proofs of existence of traveling waves by phase plane analysis. One of the simplifications made in [10] neglected the thermal capacity of the medium as compared to air. A consequence is that oxygen and heat were both transported at the speed of the moving gas. Unfortunately, the thermal capacity assumption is not correct for oil recovery and many other applications. Another simplification present in many works consists in neglecting thermal losses. Such simplification is not admissible

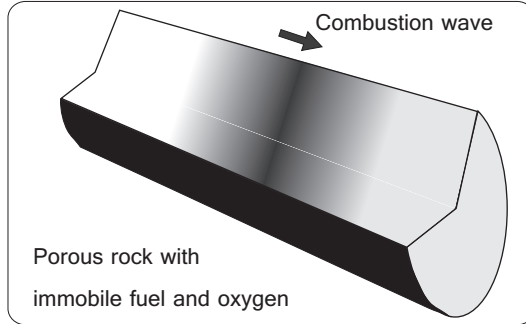


Figure 1. Sketch of in-situ combustion.

when modeling laboratory scale experiments. The third simplification used in [10] consists in considering a truncated Arrhenius law, see also [11, 12]. In this work we consider the effect of thermal losses, correct Arrhenius law and realistic thermal speed.

A model for combustion is presented in Section 2. It consists of three balance laws for energy, oxygen, and fuel. We use a reaction rate described by Arrhenius law combined with Law of Mass Action, [13][§102].

The combustion waves studied in this paper have been called “reaction-trailing smolder waves” [14] and “coflow (or forward) filtration combustion waves” [15] in the context of more realistic models of air injection into a porous medium. The moving gas brings oxygen into a region where solid fuel is present. The oxygen is consumed in the reaction. We formulate the main results of the paper in Section 3. We present the rigorous proofs about the existence and uniqueness of the combustion traveling waves in Section 4. In Section 5 some numerical examples showing the phase portrait of the traveling wave appearing in the previous sections are presented. Finally, in Section 6 some conclusions are discussed.

2. Combustion model

We consider one-dimensional flow due to air injection into a porous medium. We use notation and assumptions from [2], see Figure 1. The medium initially contains a fuel that is essentially immobile and does not vaporize, e.g., solid fuel or liquid fuel at low saturations. We assume that only a small part of the available space is occupied by fuel, so that changes of porosity during the reaction are negligible. We assume that the temperature of solid and gas is the same (local thermal equilibrium). This work is concerned with heat losses, which we consider to depend linearly on temperature difference with the prevailing temperature, see e.g., [9]. We also assume that pressure variations are small compared to the prevailing pressure, and we neglect gas expansibility under temperature increase.

The model with time coordinate t and space coordinate x includes the heat balance equation (1), the molar balance equations for oxygen (2) and immobile fuel (3). Instead of considering the Ideal Gas Law we assume that the molar density of gas ρ [mole/m³] is constant; it follows that the Darcy gas speed u [m/s] is also constant. Another simplification we will perform consists in considering the gas diffusion negligible so that there is no diffusion term in (2). The heat losses are considered linearly depending on the temperature difference with the reservoir temperature.

$$C_m \frac{\partial T}{\partial t} + \frac{\partial(c_g \rho_g u (T - T_{res}))}{\partial x} = \lambda \frac{\partial^2 T}{\partial x^2} - \alpha(T - T_{res}) + Q_r \rho Y W_r \quad (1)$$

$$\varphi \frac{\partial(Y \rho_g)}{\partial t} + \frac{\partial(Y \rho_g u)}{\partial x} = -\mu_o \rho Y W_r, \quad (2)$$

$$\frac{\partial \rho}{\partial t} = -\mu_f \rho Y W_r, \quad (3)$$

Here T [K] is the temperature, Y [mole/mole] is the oxygen molar fraction in the gas, ρ [mole/m³] is the molar concentration of immobile fuel. The system parameters together with their typical values are given in Table 1. These parameters are assumed to be constant (neglecting the dependence on temperature, gas composition, etc.), an assumption that was already used in (1).

Table 1. Dimensional parameters for in-situ combustion and their typical values.

<i>Symbol</i>	<i>Physical quantity</i>	<i>Value</i>	<i>Unit</i>
T_{res}	Initial reservoir temperature	273	[K]
C_m	Volume heat capacity of porous medium	$2 \cdot 10^6$	[J/m ³ K]
c_g	Molar heat capacity of gas	27.42	[J/mole K]
ρ_g	Average gas density	45	[mole/m ³]
λ	Thermal conductivity of porous medium	0.87	[J/(m s K)]
Q_r	Immobile fuel combustion enthalpy at T_{res}	$4 \cdot 10^5$	[J/mole]
E_r	Activation energy	58000	[J/mole]
k_p	Pre-exponential parameter	500	[1/s]
R	Ideal gas constant	8.314	[J/(mole K)]
φ	Porosity	0.3	[.]
u	Darcy velocity of injected gas (200 m/day)	$2.3 \cdot 10^{-3}$	[m/s]
ρ^{res}	Initial molar density of fuel	372	[mole/m ³]
α	Specific thermal conductivity	0.2	[J/(m ³ s K)]
Y_{inj}	Injected oxygen concentration	1.0	[.]

In the combustion reaction, μ_f moles of immobile fuel react with μ_o moles of oxygen to generate μ_g moles of gaseous products and, possibly, unreactive solid products. For simplicity, we consider the case $\mu_f = \mu_o = \mu_g = 1$ as, e.g., in the reaction $C + O_2 \rightarrow CO_2$. The reaction rate is proportional to W_r given by

$$W_r = k_p \exp\left(-\frac{E_r}{RT}\right), \quad (4)$$

where typical values of k_p and E_r also are given in Table 1.

Remark 2.1. In Table 1 the average gas density is 45 moles per cubic meter, which is close to the value for air (the molar density of CO_2 is 45, N_2 is 44, O_2 is 44.7). Physically, the difference between the two thermal conductivities (λ and α) corresponds to tube section area. Dimensional analysis confirms this idea. Thus if h is the reservoir height we have $\alpha = \lambda/h^2$. The value in the table corresponds to a reservoir with section diameter of approximately 2 meters.

2.1. Dimensionless equations

The equations are non-dimensionalized by introducing dimensionless dependent and independent variables (denoted by tildes) as ratios of the dimensional quantities and reference quantities (denoted by stars):

$$\tilde{t} = \frac{t}{t^*}, \quad \tilde{x} = \frac{x}{x^*}, \quad \tilde{\theta} = \Delta\tilde{T} = \frac{T - T_{res}}{\Delta T^*}, \quad \tilde{\rho} = \frac{\rho}{\rho^*}, \quad \tilde{Y} = \frac{Y}{Y^*}. \quad (5)$$

Our choice for reference quantities is

$$v^* = \frac{Y_{inj}\rho_g u}{\rho^{res}}, \quad t^* = \frac{1}{k_p Y_{inj}}, \quad x^* = v^* t^*, \quad \Delta T^* = \frac{Q_r \rho^{res}}{C_m}, \quad \rho^* = \rho^{res}, \quad Y^* = Y_{inj}, \quad (6)$$

where T_{res} and ρ^{res} are the initial reservoir temperature and molar density of fuel, Y_{inj} is the oxygen molar fraction in the injected gas, ρ is the average gas molar density and u is the injected gas Darcy velocity.

In (6), t^* is the characteristic time for fuel combustion at the initial reservoir temperature T_{res} ; ΔT^* is the deviation of peak temperature from reservoir temperature, for the case of complete combustion of fuel under adiabatic conditions.

Using (5), (6) and omitting the tildes, equations (1)–(4) are written in dimensionless form as follows. In order to prove rigorously the existence of traveling waves without technical difficulties we neglect the thermal diffusion effects ($\lambda = 0$). The dependent variables are temperature θ , oxygen fraction Y and fuel ρ :

$$\frac{\partial \theta}{\partial t} + v_\theta \frac{\partial \theta}{\partial x} = -\beta \theta + \rho Y \Phi, \quad (7)$$

$$\frac{\partial Y}{\partial t} + v_Y \frac{\partial Y}{\partial x} = -\mu_Y \rho Y \Phi, \quad (8)$$

$$\frac{\partial \rho}{\partial t} = -\rho Y \Phi, \quad (9)$$

$$\Phi = \exp\left(\frac{-\mathcal{E}}{\theta + \theta_0}\right) \quad (10)$$

with dimensionless constants

$$v_\theta = \frac{c_g \rho_g u}{v^* C_m}, \quad \bar{\lambda} = \frac{\lambda}{C_m v^*}, \quad \beta = \frac{\alpha t^*}{C_m}, \quad v_Y = \frac{u}{\varphi v^*}, \quad (11)$$

$$\mu_Y = \frac{k_p \rho^{inj} t^*}{\varphi \rho_g}, \quad \mathcal{E} = \frac{E_r}{R \Delta T^*}, \quad \theta_0 = \frac{T_{res}}{\Delta T^*}.$$

Here v_θ and v_Y are dimensionless thermal and oxygen waves speeds; β is the constant thermal loss coefficient; $\bar{\lambda}$ represents the dimensionless thermal diffusion coefficient; μ_Y represents the dimensionless quantity of oxygen consumed during the reaction; \mathcal{E} is the scaled activation energy and θ_0 is the scaled reservoir temperature. Typical values of the quantities in (11) are given in Section 5. The oxygen Y is a component of the gas moving with velocity $v_Y > 0$. The heat θ is transported with velocity v_θ . We are of course interested in solutions with $\rho \geq 0$ and $Y \geq 0$ everywhere. We consider (7)–(9) on $0 < x < \infty$, $t \geq 0$, with the (constant) boundary conditions

$$(\theta, \rho, Y)(0) = (\theta^L, \rho^L, Y^L), \quad (\theta, \rho, Y)(\infty) = (\theta^R, \rho^R, Y^R). \quad (12)$$

We assume that the reaction does not occur at the boundaries, i.e., the reaction terms in (7)–(9) vanish. Differently from [8, 10], here we consider the correct Arrhenius law and thus there are only two reasons for the reaction terms to vanish:

- (i) Fuel control (*FC*) – the reaction ceases due to lack of fuel, $\rho = 0$;
- (ii) Oxygen control (*OC*) – the reaction ceases due to lack of oxygen, $Y = 0$.

In the next section we study the solution of the Riemann problem of the system (7)–(9).

3. Wave sequences

In this section we follow [8, 10] and denote by $(\theta^-, \rho^-, Y^-) \xrightarrow{v} (\theta^+, \rho^+, Y^+)$ a wave of velocity v that connects (θ^-, ρ^-, Y^-) at the left to (θ^+, ρ^+, Y^+) at the right. At the end states of the wave, the reaction terms in (7)–(9) vanish. States at which the reaction terms vanish can be classified as *FC* or *OC*. The type of the state indicates exactly which conditions hold at that state. Because of the nondimensionalization we used in Section 2.1 we consider that $\rho = 1$ in *OC* state and $Y = 1$ in *FC* state.

3.1. Contact waves

In the non-combustion waves supported by system (7)–(9) the source terms vanish. The characteristic eigenvalues and corresponding eigenfunctions of the resulting hyperbolic system are [10]:

$$\begin{aligned} \lambda_\theta &= v_\theta; & (1, 0, 0)^T; \\ \lambda_Y &= v_Y; & (0, 1, 0)^T; \\ \lambda_f &= 0; & (0, 0, 1)^T. \end{aligned} \tag{13}$$

We can see that the Riemann problem possesses three non-combustion contact waves. As the characteristic velocities are constant they correspond to contact discontinuity waves, see [16]. Contact discontinuities must separate moving spatial intervals in which the reaction does not occur (since (θ, ρ, Y) is constant). The waves in a wave train must occur in order of increasing velocity from left to right.

3.2. Combustion waves

As in [10], system (7)–(9) possesses a combustion wave. We formulate the main result below and prove it in Section 4.

Theorem 3.1. *The system (7)–(9) possesses a unique traveling combustion wave in the following cases*

- (i) *If $v_Y < (\mu_Y + 1)v_\theta$ then a slow combustion wave with speed $v < v_\theta$ exists.*
- (ii) *If $v_Y > (\mu_Y + 1)v_\theta$ then a fast combustion wave with speed $v > v_\theta$ exists.*
- (iii) *If $v_Y = (\mu_Y + 1)v_\theta$ then there exists a combustion wave if and only if: either $\mathcal{E} < 4\theta_0$ or there are exactly three values of $\theta > 0$ satisfying Eq. (30), namely $4f(\theta) = 1$.*

In all cases the combustion wave is of type $FC \xrightarrow{v} OC$, where its velocity is given by Eq. (17).

3.3. Solutions of the Riemann problem

An obvious necessary condition for the existence of a wave sequence describing Riemann solution is that it has to start as one equilibrium state (*FC* or *OC*) and finish at another equilibrium state (*FC* or *OC*). The waves speeds in the sequence appear in increasing order from left to right. This fact together with the results concerning contact and combustion waves described above lead to three possibilities for wave sequences corresponding respectively to three cases described in Theorem 3.1.

- (i) *If the sequence contains a slow combustion wave $FC \xrightarrow{v} OC \xrightarrow{v_\theta} OC$.*
- (ii) *If the sequence contains a fast combustion wave $FC \xrightarrow{v_\theta} FC \xrightarrow{v} OC$.*
- (iii) *If the sequence is composed of a single resonance combustion wave $FC \xrightarrow{v} OC$.*

In Fig. 2 we plot the wave sequences separated by constant states for the cases (i) (left figure), (ii) (center figure) and (iii) right figure. Notice that θ^b indicate the temperature of the combustion wave.

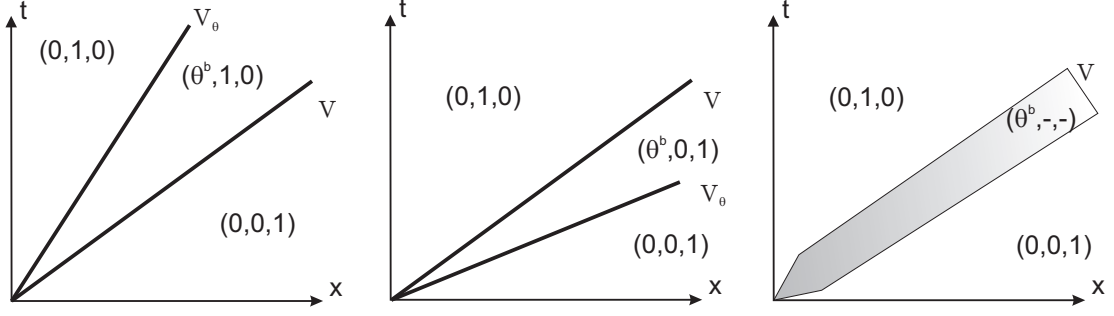


Figure 2. Wave sequences in Riemann solution separated by constant states for the cases (i) (left figure), (ii) (center figure) and (iii) right figure.

4. Existence and uniqueness of the combustion traveling waves

We rewrite the system (7)-(9) in traveling coordinates $(x, t) \rightarrow (\xi = x - vt, t)$, where v is positive velocity of the traveling wave

$$-v\partial_\xi\theta + v_\theta\partial_\xi\theta = -\beta\theta + \rho Y\Phi, \quad (14)$$

$$-v\partial_\xi Y + v_Y\partial_\xi Y = -\mu_Y\rho Y\Phi, \quad (15)$$

$$-v\partial_\xi\rho = -\rho Y\Phi. \quad (16)$$

Substituting (16) into (15), integrating in ξ from $-\infty$ to ∞ and using the boundary conditions (12) yields

$$v = \frac{v_Y}{\mu_Y + 1}. \quad (17)$$

Notice that this formula allows to classify the velocity of the combustion wave appearing in the statement of Theorem 3.1. Substituting (16) into (15), integrating from ξ to the boundary condition at $\xi \rightarrow \infty$ we obtain

$$Y = 1 - \rho. \quad (18)$$

Thus the system (14)–(16) can be rewritten as two ODEs

$$\partial_\xi\rho = \rho(1 - \rho)\frac{\Phi}{v}, \quad (19)$$

$$\partial_\xi\theta = \frac{\rho(1 - \rho)\Phi - \beta\theta}{v_\theta - v}. \quad (20)$$

In the calculations that follow we consider the case when $v_\theta \neq v$. The case when $v_\theta = v$ is known as resonance condition for the combustion wave, see [15, 17, 4] and references therein. We study this case separately in Proposition 4.3.

The linearization of the system (19)–(20) at the point (ρ, θ) yields the matrix of derivatives

$$DF = \begin{bmatrix} \frac{1 - 2\rho}{v}\Phi & \rho(1 - \rho)\frac{\mathcal{E}}{(\theta + \theta_0)^2}\frac{\Phi}{v} \\ \frac{1 - 2\rho}{v_\theta - v}\Phi & \frac{1}{v_\theta - v}\left(\rho(1 - \rho)\frac{\mathcal{E}}{(\theta + \theta_0)^2} - \beta\right) \end{bmatrix}. \quad (21)$$

At OC and FC equilibria the matrix DF has the forms:

$$DF_{OC} = \begin{bmatrix} -\frac{e}{v} & 0 \\ -\frac{e}{v_\theta - v} & \frac{-\beta}{v_\theta - v} \end{bmatrix}, \quad DF_{FC} = \begin{bmatrix} \frac{e}{v} & 0 \\ \frac{e}{v_\theta - v} & \frac{-\beta}{v_\theta - v} \end{bmatrix}, \quad (22)$$

where $e = \exp(-\mathcal{E}/\theta_0) > 0$. The corresponding eigenvalues and eigenvectors are

$$\lambda_{OC}^1 = -\frac{e}{v} < 0, \quad \left[\frac{v_\theta - v}{v} - \frac{\beta}{e}, 1 \right]^T; \quad (23)$$

$$\lambda_{OC}^2 = \frac{\beta}{v - v_\theta}, \quad [0, 1]^T;$$

$$\lambda_{FC}^1 = \frac{e}{v} > 0, \quad \left[\frac{v_\theta - v}{v} + \frac{\beta}{e}, 1 \right]^T; \quad (24)$$

$$\lambda_{FC}^2 = \frac{\beta}{v - v_\theta}, \quad [1, 0]^T.$$

Following [10], waves with velocities $v > v_\theta$ and $v < v_\theta$ are called *fast combustion wave* and *slow combustion wave* respectively. We analyze them below.

Proposition 4.1. *Exists a unique slow combustion traveling wave solution for the system (7)–(10).*

Proof. Using $v < v_\theta$ in Eqs. (23)–(24) we notice that the matrix of derivatives at OC equilibrium possesses two negative eigenvalues, thus OC is a sink. The equilibrium FC is a saddle. It follows that the only possible combustion wave is $FC \xrightarrow{v} OC$.

Let us study the phase portrait in (ρ, θ) space. The horizontal component of the vector field of (19)–(20) is strictly positive between the lines $\rho = 0$ and $\rho = 1$, which are invariant manifolds for this field. The vertical component of the vector field of (19)–(20) is discussed in Section 4.1. These fields are plotted schematically in Fig. 3.

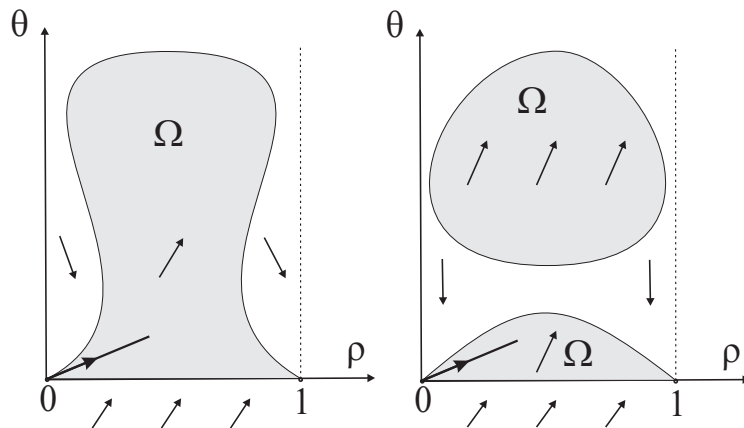


Figure 3. Phase space of the system (19)–(20) for the slow combustion wave with equilibria FC at $(0, 0)$ and OC at $(1, 0)$. Left: Case 1. Right: Case 2.

The tangent direction to the curve Γ at the equilibrium FC is $(1, e/\beta)$ and the eigenvector corresponding to the positive eigenvalue λ_{FC}^1 has smaller slope than this direction, see Fig. 3.

Thus, at least some part of the unstable manifold of FC stays inside the region Ω where the vertical component of the field is negative. As Ω is compact this manifold crosses Γ at some point P . The orbit starting at P is attracted to the sink OC , see Fig. 3. This proves the existence of the heteroclinic orbit leaving FC and reaching OC . Uniqueness of this wave follows from the hiperbolicity of the FC equilibrium. \square

Proposition 4.2. *Exists a unique fast combustion traveling wave solution for the system (7)–(10).*

Proof. Using $v > v_\theta$ in Eqs. (23)–(24) we notice that the matrix of derivatives at the equilibrium FC possesses two positive eigenvalues, thus FC is a source. On the other hand the equilibrium OC is a saddle. The only possible combustion wave is $FC \xrightarrow{v} OC$.

Let us study the phase portrait in (ρ, θ) space. Analogously to the slow combustion case, the horizontal component of the vector field of (19)–(20) is strictly positive between the lines $\rho = 0$ and $\rho = 1$, which are therefore invariant manifolds for this field. The vertical component of the vector field of (19)–(20) is discussed in Section 4.1. These fields are schematically plotted in Fig. 4.

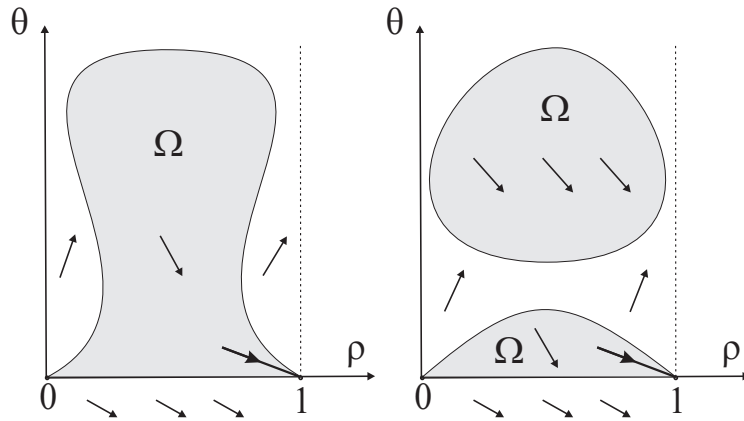


Figure 4. Phase space of the system (19)–(20) for the fast combustion wave with equilibria FC at $(0,0)$ and OC at $(1,0)$. Left: Case 1. Right: Case 2.

The tangent direction to the curve Γ at the equilibrium OC is $(1, -e/\beta)$ and the eigenvector corresponding to the positive eigenvalue λ_{OC}^1 has less negative slope than this direction, see Fig. 4. Thus, at least some part of the stable manifold of OC stays inside the region Ω where the vertical component of the field is negative. As Ω is compact this manifold crosses Γ at some point P . The orbit reaching P is attracted to the source OC for negative times, see Fig. 4. This proves the existence of the heteroclinic orbit reaching OC from FC . Uniqueness of this wave follows from the hiperbolicity of the OC equilibrium. \square

Proposition 4.3. *For the resonance case $v = v_\theta$, exists a unique combustion traveling wave solution for the system (7)–(10) if and only if either $\mathcal{E} < 4\theta_0$ or Eq. (30) is satisfied for exactly three values of θ .*

Proof. In the case $v_\theta = v$, instead of the system (19)–(20) we obtain:

$$\partial_\xi \rho = \rho(1 - \rho)\Phi/v, \quad (25)$$

$$f(\theta) = \rho(1 - \rho). \quad (26)$$

The horizontal component of the flux of this system is strictly positive and the orbit stays on the curve Γ described in Section 4.1. Thus there is an orbit connecting equilibria FC and OC if

- there exists a continuous part of Γ connecting FC and OC called Γ_c and
- the horizontal component of the flux stays positive along Γ_c .

This can happen in two situations (see Section 4.1): for the geometry corresponding to Case 1 if $\mathcal{E} > 4\theta_0$ and any local map $\rho(\theta)$ of Γ_c does not possess critical points, see left part of Fig. 5; or for the geometry corresponding to Case 2 (i.e., there are three values of $\theta > 0$, such that $4f(\theta) = 1$), see right part of Fig. 5. The proof of the uniqueness of this wave is trivial. \square

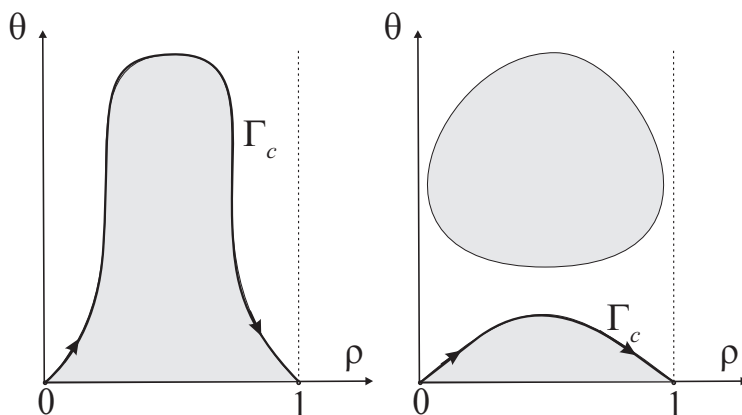


Figure 5. Phase space of the system (25)–(26) for the resonance combustion wave with equilibria FC at $(0,0)$ and OC at $(1,0)$. Left: Case 1. Right: Case 2.

4.1. The curve Γ

The vertical component of the vector field of (19)–(20) changes sign together with the term $\rho(1-\rho)\Phi - \beta\theta$, which is a continuous function in θ . Let us define the curve Γ as the geometrical place where this term is equal to zero

$$\Gamma = \{(\rho, \theta) : \rho(1-\rho) = f(\theta), \theta \geq 0\}, \quad \text{where} \quad f(\theta) = \beta\theta \exp\left(\frac{\mathcal{E}}{\theta + \theta_0}\right). \quad (27)$$

Notice that Γ contains both equilibria OC and FC . If $(\rho, \theta) \in \Gamma$, then

$$\rho = \frac{1 \pm \sqrt{1 - 4f(\theta)}}{2}. \quad (28)$$

Inspecting function $f(\theta)$ we notice that $f(\theta) \geq 0$, $f(0) = 0$, $\lim_{\theta \rightarrow \infty} f(\theta) = \infty$ and has two extremal points

$$f'(\theta^c) = 0 \implies (\theta^c + \theta_0)^2 - \theta^c \mathcal{E} = 0 \implies \theta_{\pm}^c = \frac{\mathcal{E} - 2\theta_0 \pm \sqrt{\mathcal{E}^2 - 4\mathcal{E}\theta_0}}{2}. \quad (29)$$

It is easy to see that if $\mathcal{E} \leq 4\theta_0$ then $f(\theta)$ possesses either 0 or 1 critical points, thus $f(\theta)$ is monotonic and for each ρ there is exactly one value of θ on Γ . If $\mathcal{E} > 4\theta_0$ Eq. (29) yields two critical points for $f(\theta)$. It is easy to see that $\theta_+^c > \theta_-^c > 0$. Thus there are either one or tree values of θ for which

$$4f(\theta) = 1 \quad (30)$$

is satisfied. We can study two separate cases:

- **Case 1:** Equation (30) is satisfied for exactly one value of θ .
- **Case 2:** Equation (30) is satisfied for exactly three values of θ .

Remark 4.4. Notice that in the model (7)–(9) without thermal losses the traveling wave equations under the resonance condition $v = v_\theta$ result in a degenerate traveling wave without combustion. The same situation happens for the model studied in [10]. Thus taking into account thermal losses allows the appearance of a different type of solution, which is interesting from the physical point of view.

Remark 4.5 (Bifurcation between case 1 and case 2). The bifurcation point between cases 1 and 2 happens when there is exactly one valid value of θ satisfying $4f(\theta) = 1$. It can be obtained implicitly from Eq. (29):

$$\theta_- = \frac{\mathcal{E} - 2\theta_0 - \sqrt{\mathcal{E}^2 - 4\mathcal{E}\theta_0}}{2}; \quad \beta\theta_- = \frac{1}{4} \exp\left(\frac{-\mathcal{E}}{\theta_- + \theta_0}\right) \quad (31)$$

We conjecture that for more complicated models this bifurcation evolves to the separation between stable hot and unstable cold combustion waves, see [9].

5. Numerical Example

Substituting the values from Table 1 into Eq. (11) one obtains:

$$\begin{aligned} v_\theta = 0.0051, \quad \bar{\lambda} = 0.00156, \quad \beta = 2 \cdot 10^{-10}, \quad v_Y = 2.76, \\ \mu_Y = 2.76, \quad \mathcal{E} = 93.8, \quad \theta_0 = 3.67. \end{aligned} \quad (32)$$

For the values of Table 1 we plot the curve Γ numerically in Figure 6 for Cases 1 and 2 as explained in Section 4.1.

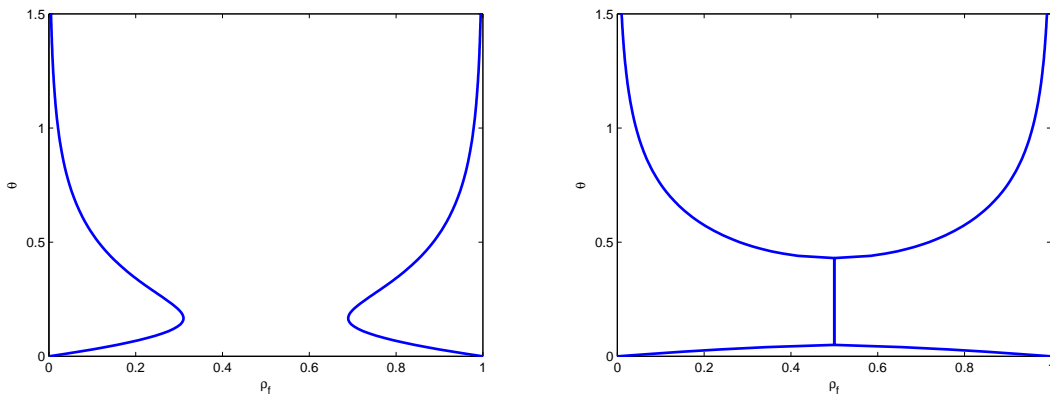


Figure 6. Phase portrait of the system (19)–(20) obtained numerically. Case 1 geometry is plotted on the left. Case 2 geometry is plotted on the right.

We can obtain a numerical approximation of the heteroclinic orbit by starting close to the saddle point and integrating toward negative time as shown in Figure 7.

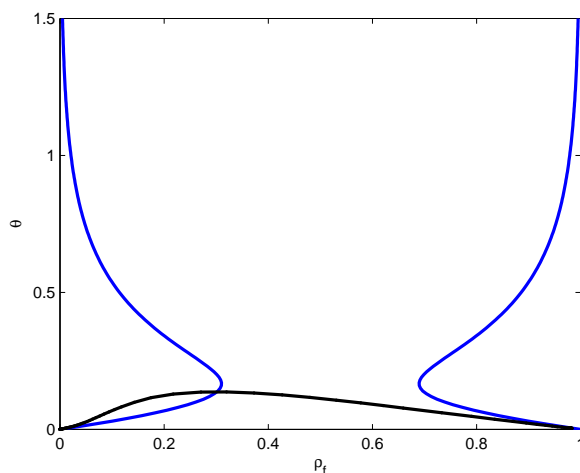


Figure 7. Phase portrait of the system (19)–(20) with heteroclinic orbit corresponding to the fast combustion wave in Case 1.

6. Conclusions

In this paper we prove the existence of a traveling wave solution corresponding to the combustion wave for a simple in-situ combustion model. This model is more general than the previously considered one [10] in three aspects. First it considers more physically realistic thermal capacity of the medium, leading to different thermal and gas velocities. Second, we consider more correct Arrhenius law allowing chemical reaction to happen at any temperatures. Third, we take into account thermal losses effect, which is important for laboratory experiments.

We solved possible Riemann problems and classified the obtained solutions depending on the presence of slow, fast or resonance combustion waves. We emphasize that the existence and uniqueness proofs presented in this paper are technically simple and should be accessible to undergraduate and master students.

Acknowledgments

The authors would like to thank Prof. S. Schechter (NCSU), L. Furtado (U. Columbia) and F. Ozbag (NCSU) for preliminary work.

G.C. was supported in part by CNPq, FAPEMIG and CAPES.

D.M. was supported in part by: ANP–PRH32 under grant 731948/2010; Petrobras–PRH32 under grant 6000.0069459.11.4; CAPES Nuffic under grant 024/2011; CNPq under grants 402299/2012-4, 301564/2009-4, 470635/2012-6; FAPERJ under grants E-26/210.738/2014, E-26/201.210/2014, E-26/110.658/2012, E-26/111.369/2012, E-26/110.114/2013, E-26/010.002762/2014.

References

- [1] Bruining J, Mailybaev A and Marchesin D 2009 *SIAM Journal on Applied Mathematics* **70** 1157–1177
- [2] Chapiro G, Mailybaev A A, Souza A, Marchesin D and Bruining J 2012 *Comput. Geosciences* **16** 799–808
- [3] Mailybaev A, Bruining J and Marchesin D 2011 *Combustion and Flame* **158** 1097–1108
- [4] Mailybaev A, Marchesin D and Bruining J 2011 *SIAM Journal on Mathematical Analysis* **43** 2230–2252
- [5] Marchesin D and Schechter S 2003 *Zeitschrift für Angewandte Mathematik und Physik (ZAMP)* **54** 48–83
- [6] Mota J and Schechter S 2006 *Journal of Dynamics and Differential Equations* **18** 615–665
- [7] Schechter S and Marchesin D 2001 *Bulletin of the Brazilian Mathematical Society* **32** 237–270
- [8] Chapiro G, Furtado L, Marchesin D and Schechter S 2015 *Accepted in DCDS*

- [9] Akkutlu I and Yortsos Y 2003 *J. of Combustion and Flame* **134** 229–247
- [10] Chapiro G, Marchesin D and Schechter S 2014 *Journal of Hyperbolic Differential Equations* **11** 295–328
- [11] Souza A J, Marchesin D and Akkutlu I Y 2006 *Comp. Appl. Math* **25** 27–54
- [12] Chapiro G and de Souza A J 2015 *Applicable Analysis* 1–15
- [13] Landau L and Lifshitz E 1980 *Statistical Physics, Vol 5 (Course of theoretical physics)* 3rd ed (Pergamon)
- [14] Schult D, Matkowsky B, Volpert V and Fernandez-Pello A 1996 *Combustion and Flame* **104** 1–26
- [15] Aldushin A, Rumanov I and Matkowsky B 1999 *J. of Combustion and Flame* **118** 76–90
- [16] LeVeque R J 1992 *Numerical methods for conservation laws* vol 132 (Springer)
- [17] Chapiro G and Bruining J 2015 *Journal of Petroleum Science & Engineering* **127** 179–189